# Aircraft study of secondary aerosols in long-range transported air masses from the North China Plain by a mid-latitude cyclone

**Peng Sun[1,2*], Wei Nie[1,2], Xuguang Chi[1,2], Xin Huang[1,2], Chuanhua Ren[1,2], Likun Xue[2,3], Ye Shan[3], Liang Wen[3,†], Hongyong Li[3], Tianshu Chen[3], Yanbin Qi[4,5], Jian Gao[6], Qi Zhang[7] and Aijun Ding[1,2*]**

[1] Joint International Research Laboratory of Atmospheric and Earth System Sciences, School of Atmospheric Sciences, Nanjing University, Nanjing 210023, China.

[2] Jiangsu Provincial Collaborative Innovation Center for Climate Change, Nanjing 210023, China.

[3] Environment Research Institute, Shandong University, Ji'nan, Shandong, China

[4] Jilin Province Technology Center for Meteorological Disaster Prevention, Changchun 130062

[5] Joint Open Laboratory for Weather Modification of China Meteorological Administration/People's Government of Jilin Province, Changchun 130062, China;

[6] State Key Laboratory of Environmental Criteria and Risk Assessment, Chinese Research Academy of Environmental Sciences, Beijing, China

[7] Department of Environmental Toxicology, University of California, 1 Shields Ave., Davis, CA 95616, USA

Corresponding author: Peng Sun (sunpeng@nju.edu.cn); Aijun Ding (dingaj@nju.edu.cn)

[†] Now at Leibniz-Institute for Tropospheric Research (TROPOS), Atmospheric Chemistry Department (ACD), Permoserstraße 15, 04318 Leipzig, Germany

Key Points:

- Aircraft measurements recorded high loadings of sulfate-dominated secondary aerosols in the free troposphere of the Northeast China.
- Strong changes of secondary aerosols occurred in the fronts-induced air masses transported by a mid-latitude cyclone.
- Increased sulfate contribution in $PM_{2.5}$ was mainly caused by evaporation-induced nitrate losses during the transport.
-

Abstract

Regional transport has been identified as an important contributor to air pollution. Yet, understanding evolution of aerosol components associated with synoptic systems remains limited, particularly in China, where most of the measurement studies were conducted at ground-surface. In this study, an intensive

campaign was designed with an aircraft measurement in Northeast China (NEC) together with ground-surface measurements in North China Plain (NCP), to investigate the role that the mid-latitude cyclone plays in transporting air pollution, specifically in changing aerosol components during the transport. During a flight on 30 July 2018, high concentrations of aerosols dominated by sulfate were observed in the free troposphere (FT), despite low aerosol loadings dominated by organics in the planetary boundary layer. Model simulations indicated that pollution in the lower free troposphere (LFT) was transported directly from North Hebei by warm and moist air masses, while pollution in the higher free troposphere (HFT) was influenced by the warm conveyor belt (WCB), which transported aerosols from the NCP and lifted them into the HFT. Both particulate nitrate and sulfate were formed productively due to strong emissions and high atmospheric oxidizing capacity in the NCP. During the transport, sulfate concentrations stayed relatively constant while nitrate decreased readily due to evaporation losses, resulting in an increasing contribution of sulfate but a decreasing contribution of nitrate to secondary aerosols along the transport path.

**Plain Language Summary**

Atmospheric chemical processes may occur inside an air mass plume as it moves continuously along the trajectory. This challenges the signal-site based investigation in understanding the change of aerosol composition. Here, we organized a campaign using an aircraft in the Northeast China (NEC) and multiple ground observations in North China Plain (NCP) to investigate aerosol chemistry during the regional transport from the NCP to the NEC influenced by a mid-latitude cyclone. High loadings of aged secondary aerosols observed in the free troposphere in the NEC were attributed to the regional transport from the NCP. Both sulfate and nitrate formed strongly in the NCP but behaved differently during the transport to the north in that sulfate kept constant while nitrate decreased readily due to evaporation losses.

## 1 Introduction

Atmospheric aerosols, especially fine particles ($PM_{2.5}$, aerodynamic diameter 2.5 m), have adverse effects on human health (Wang et al., 2012; Zhang et al., 2015), reduce visibility (Charlson and Heintzenberg, 1995), and influence climate and ecosystems (Ellison et al., 2020). Therefore, full characterization of the sources, chemical compositions, and evolution processes of atmospheric aerosols is crucial to elucidate the effects they cause. Extensive field studies around the world have investigated the chemical properties of $PM_{2.5}$, and usually found that organics and secondary inorganic species, i.e., sulfate, nitrate and ammonium (SNA), were the dominant aerosol components (Jimenez, et al., 2009; Zhang et al., 2007; Huang et al., 2014; Li et al., 2017b; Zhou et al., 2020). The mass concentrations and compositions of fine particles show dramatic temporal and spatial variations due to influences from various emission sources, atmospheric processes, and meteorological conditions (Li et al., 2017b; Kim et al., 2017).

The particulate pollution of a specific area is contributed by both its local sources and regional transport processes, which sometimes have been identified as a main reason for the occurrence of regional haze episodes (Sun et al., 2014; Sun et al., 2020; Huang et al., 2020; Wang et al., 2020; Kim et al., 2018; Dong et al., 2018). Du et al. (2020) conducted model simulations and illustrated the importance of transported secondary aerosols and precursors on haze in the North China Plain (NCP). Zhang et al. (2021) carried out field studies and investigated compositions and aging of haze aerosols during the trans-regional transport from NCP to Yangtze River Delta (YRD). Tan et al. (2021) even found an increasing impacts of the relative contributions of regional transport on surface air pollution in Beijing through observational evidence. A Common view has been reached that coordinated cross-regional emission reduction strategy is required to further mitigate haze pollution. Though previous studies have emphasized the importance of regional transport on aerosol loadings and frequent haze episodes, they were focused on the aerosols within planetary boundary layer (PBL) based on the ground observations and corresponding simulations.

The PBL into free troposphere (FT) transport is of great importance for the understanding of atmospheric chemistry and climate issues (Henne et al., 2005), but scant research has covered this topic. Partially because both airborne and ground observations are simultaneously required to fully capture the composition and evolution of aerosols, which challenges the observation technology. The frontal systems, especially the so-called warm conveyor belts (WCBs), associated with cyclones are the dominant mechanism that could lift or ventilate PBL air into the FT (Bethan et al., 1998). Air pollutants, including ozone, aerosols, and their precursors, can substantially change the chemical environment and radiation property of the troposphere. The longer lifetime of these pollutants in the FT extends their impact from the regional to the continental or even global scale because of long-range transport (Henne et al., 2005; Dickerson et al., 2007; Ding et al., 2009).

North China Plain (NCP), which includes the Beijing and Tianjin city clusters and many other cities in the flat region of central-eastern China, experiences severe air pollution owing to high population density, intense industrial activities, and unfavorable meteorology conditions in the region (Wang et al., 2006; Hu et al., 2017; Sun et al., 2013; Li et al., 2017; Sun et al., 2014; Zhang et al., 2016; Wang et al., 2017). The NCP thus serves as an important pollution source region, from where polluted air masses are easy to be transported to other regions through different synoptic systems. For example, air pollutants transported from NCP to YRD have been fully investigated (Ding et al., 2013; Sun et al., 2020; Huang et al., 2020; Wang et al., 2020; Chen et al., 2020b; Bao et al., 2017).

Northeast China (NEC) is easily influenced by the northward transport of pollutants accumulated in the NCP through synoptic systems (Ma et al., 2018; Li et al., 2019) and thus becomes an ideal region to study this PBL to FT transport.

Lots of studies have emphasized the important role that mid-latitude cyclones play in exporting air pollution from the NCP to the NEC (Eckhardt et al., 2004; Stohl, 2001; Li et al., 2012; Dickerson et al., 2007; Oshima et al., 2013; Ding et al., 2009; Wu et al., 2018). However, the understanding of the detailed transport mechanism and the aerosol chemistry during the transport remains poor. This mid-latitude cyclone-influenced regional air transport can lift pollution plumes into FT from PBL (Bethan et al., 1998; Fuelberg, 2006; Cooper et al., 2004; Stohl et al., 2003). Thus both aircraft and multiple ground measurements are required to investigate the evolution of aerosol chemistry along the transport path.

In this study, we organized a campaign to conduct multiple-platform measurements of chemically-resolved $PM_{2.5}$. Specifically, we conducted aircraft measurements in the NEC using a Time-of-Flight Aerosol Chemical Speciation Monitor (ToF-ACSM) to capture the air plume over the downwind region, and we also conducted multiple ground measurements using Monitor for Aerosols and Gases in ambient air (Marga) in the NCP to measure aerosol chemical compositions in the source regions and along the transport path. To provide a regional picture of the air pollution distribution, the monthly average $SO_2$ concentrations in July 2018 in eastern China are shown in Fig. 1a. A flight was specifically designed in late July to investigate the role that a mid-latitude cyclone plays in air pollution transport. By combining Lagrangian dispersion modeling and WRF-Chem (the Weather Research and Forecasting model coupled with Chemistry) numerical simulations, we present a detailed analysis of the PBL to FT long-range transport of air pollutants and the evolution of aerosol chemistry alongside.

## 2 Materials and Methods

2.1 Aircraft and multiple ground measurements

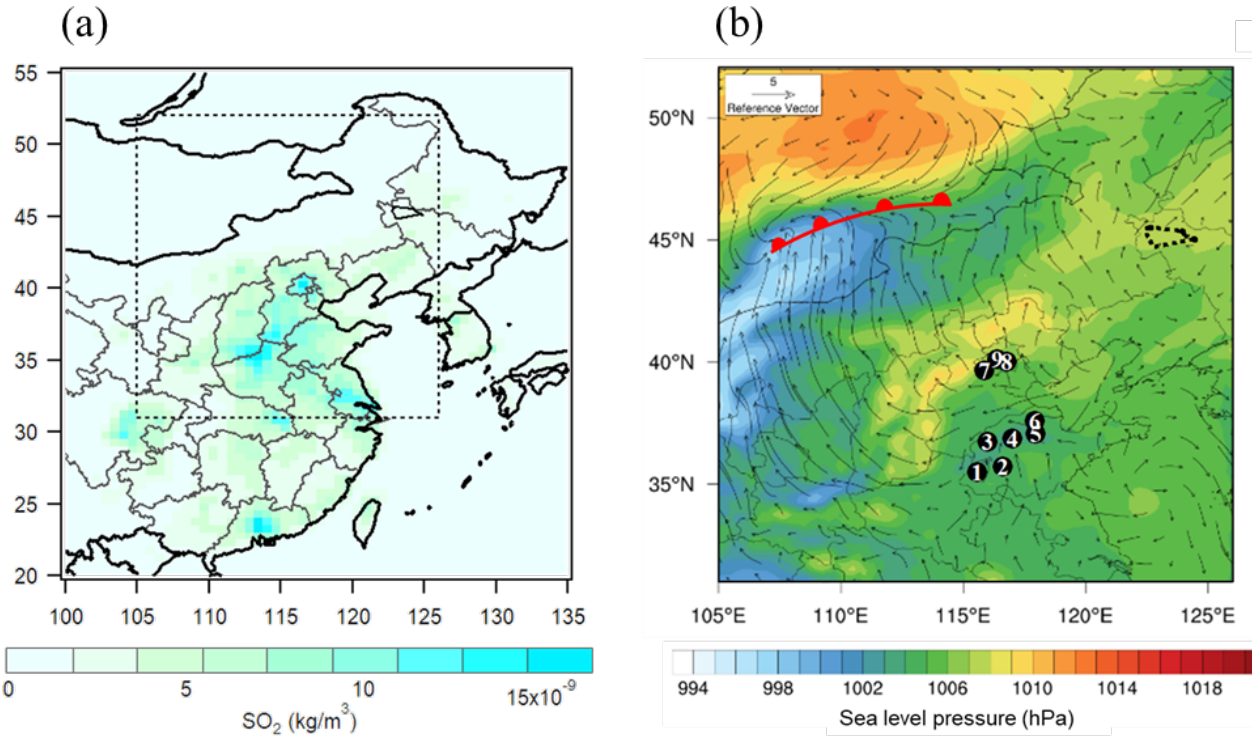


**Figure 1** (a) Map showing the distribution of average surface $SO_2$ mass concentrations in July in eastern China from OMI satellite reproduced dataset . (b) Measurement overview. Map showing the surface measurement sites (black circles with white numbers) and flight route (black dotted lines). The numbers from 1 to 9 correspond to the measurement sites in Heze, Jining, Liaocheng, Jinan, Zibo, Binzhou and 3 sites in Beijing. The spatial distributions of sea level pressure and 10-m wind field at 16:00 LT on July 28, 2018 are also shown corresponding to the areas in the black box marked in (a). The surface position of the warm front is marked with the symbol of a red line with semicircles. The meteorology data were downloaded from the ERA5 reanalysis website.

We conducted aircraft measurements of trace gases and aerosols from July to August 2018 in Jilin province of NE China. A Y-12 aircraft of the Jilin Weather Modification Office was used for the study. This twin-engine turboprop aircraft was similar to a Twin Otter. The aircraft campaign was conducted out of Baicheng city (122.84°E, 45.63°N), which is located 300 km from Changchun (the capital of Jilin, with a population of 7 million). The airport is located in the north (generally upwind direction) of the city. The sampling inlet was mounted at the bottom of the airframe with a forward-facing inlet connected to the measurement instruments. $O_3$ and $SO_2$ were measured with Thermo instruments (TEI 49i and 43i), and the aerosol scattering coefficients were measured

with a commercial integrating nephelometer (TSI3563), which detects the light scattering coefficient (Bsp) at 450 nm, 500 nm, and 700 nm. All trace gas instruments were calibrated at the ground base and different altitudes on several selected flights. An Aerodyne time-of-flight Aerosol Chemical Speciation Monitor (TOF-ACSM) (Fröhlich et al., 2013; Sun et al., 2020) was deployed and fixed in the aircraft cabin for the chemical characterization of non-refractory $PM_{2.5}$ (NR-$PM_{2.5}$). The detailed descriptions and data analysis of the instrument are in Text S1.

For multiple-surface measurements, the inorganic ions of $PM_{2.5}$ were measured with a Monitor for Aerosols and Gases in ambient Air (MARGA, designed and manufactured by Applikon Analytical B.V., the Netherlands) (ten Brink et al., 2007) at 9 ground supersites in the NCP with three in the megacity Beijing and the other six in the Shandong Province, located from South to North in Heze, Jining, Liaocheng, Jinan, Zibo, and Binzhou, separately (Fig. 1b).

2.2 Designed aircraft experiments under the influence of mid-latitude cyclone

Previous studies have indicated the important role of mid-latitude cyclone in transporting pollutants from the NCP to NE China (Eckhardt et al., 2004; Stohl, 2001; Li et al., 2012; Dickerson et al., 2007; Oshima et al., 2013; Ding et al., 2009; Wu et al., 2018). In this study, we specially designed an aircraft experiment on July 30, 2018 under the influence of a cyclone. As shown in Fig. 1b, a deep mid-latitude cyclone was located over Mongolia (centered at 107°E, 45°N). The cyclone was characterized by a low-pressure system on the ground with a warm front extending from the center to the western edge of inner Mongolia. Wind vectors clearly show that warm and humid air from the NCP moved northwardly until encountered cold air mass from the north Mongolia and accordingly formed the convergence belt. Previous studies have identified the warm conveyor belt (WCB) from the distribution of 500 hPa specific humidity due to moisture advection associated with the lifting effect (Kiley and Fuelberg, 2006; Ding et al., 2009). The 500 hPa specific humidity field (Fig. S1) consistently shows a moist band over the front, revealing the strong vertical venting in this region. The distribution of specific humidity and wind filed indicate that a WCB-like circulation extended from the warm sector of the frontal system to NE China, where we conducted our aircraft study.

In addition to this specially designed experiment, we have also conducted 4 aircraft experiments respectively on August 2, August 3, August 8 and August 9. All the experiments were carried out during the daytime.

2.3 Positive matrix factorization (PMF)

Positive matrix factorization (PMF) (Paatero and Tapper, 1994) with the PMF2.exe algorithm was performed on the TOF-ACSM organics mass spectra to investigate various organic aerosol (OA) sources and processes. PMF analysis was performed with an Igor Pro-based PMF Evaluation Tool (Ulbrich et al., 2009), and the results were evaluated following the procedures detailed in Ulbrich et al. (2009) and Zhang et al. (2011). The total OA of all aircraft

experiments was resolved into a hydrocarbon-like OA (HOA) factor and an oxygenated OA (OOA) factor. The detailed PMF results are described in Text S2.

2.4 The WRF-Chem model

The WRF-Chem model is an online-coupled chemical transport model that considers multiple physical and chemical processes, including emission and deposition of pollutants, advection, diffusion, gaseous chemical transformation, and aerosol chemistry (Grell et al., 2011). In this study, the WRF model (version 3.9.1) was employed to simulate weather conditions using the 1° x 1°NCEP (National Centers for Environmental Prediction) FNL Operational Global Analysis data (ds083.2). Meanwhile, the NCEP ADP Global Upper Air Observational Weather Data (ds351.0) was assimilated to improve the model's meteorological reproduction.

The simulation is conducted from 1 July 2018 to 20 August 2018. The detailed configurations of the model are listed in Table S1. In this study, the model domain was centered at 35° N and 110° E with a 20 km × 20 km spatial resolution to cover the eastern China and its surrounding areas. On vertical distribution, 30 vertical layers are set from the surface to the top pressure of 50 hPa, and 10 of which are set below 1 km to better resolve the processes within boundary layer. Natural emissions such as biogenic, sea salt and dust are included online into the model runs for this study. For biogenic emissions, online biogenic emissions are calculated through MEGAN (Model of Emissions of Gases and Aerosols from Nature) module. It estimates the net emission rates of isoprene, monoterpene and other biogenic VOCs from terrestrial ecosystems into the above-canopy atmosphere. In addition to natural emissions, the anthropogenic emissions of CO, $NO_x$, $SO_2$, $NH_3$, BC, OC, $PM_{2.5}$. $PM_{10}$ and VOCs are set based on the MEIC database (Multi-resolution Emission Inventory for China) (Huang et al., 2018).

To investigate the contributions of each individual physical and chemical process to variations of atmospheric nitrate and sulfate concentrations, we performed a diagnostic analysis in WRF-Chem modeling (Wang et al., 2020). The detailed diagnostic analysis and model evaluation are described in Text S3.

2.5 Lagrangian dispersion modeling

Lagrangian particulate dispersion modeling (LPDM) was used to study the transport pathways and trace the potential sources of air masses during the campaign using HYSPLIT (Stein et al., 2015), following the method developed by Ding et al. (2013). Briefly, for each hour during the study period, the model was run several days backwardly with 3,000 particles released every hour at a specific height over the site. The model calculated the particle position with mean wind and turbulent transport after being released from the receptor point. The residence time of particles at specific height columns was used to identify the footprint retroplume. The spatiotemporal distributions of these particles were used to identify the potential source regions and their relative contributions to the air masses at the measurement sites.

## 3. Results and discussions

3.1 Overall aircraft observation results

Fig. 2 shows the overall results of these 5 aircraft experiments conducted in the NEC. The overall NR-$PM_{2.5}$ was dominated by secondary species, including sulfate, ammonium, nitrate and OOA since most of the flight time is outside the boundary layer, where the influence of surface primary emission is supposed to be small. Pollution episodes were captured by our flight on July 30 and August 3 with relatively higher mass concentrations of NR-$PM_{2.5}$.

Sulfate, a secondary inorganic specie usually formed over a regional scale (Sun et al., 2011) contributed a significant fraction of NR-$PM_{2.5}$ on July 30 (43%) and August 3 (54%). The sulfur oxidation ratios (defined as $SOR = nSO_4^{2-} / (nSO_4^{2-} + nSO_2)$, where n represents molar concentration) were substantially higher on these two days, indicative of overall aged secondary aerosols. HOA, which represents primary organic aerosols (POA) usually associated with freshly traffic emissions (Zhang et al., 2011), contributed notably to NR-$PM_{2.5}$ mass loadings during clean situations and its contribution were comparable on August 2 (13%), August 8 (15%) and August 9 (17%). While extremely lower contributions of HOA and relatively higher SOA to POA ratios were observed on pollution days, indicating the possible influence of regional transport rather than local sources. $f_{m/z}$ is defined as the fraction of the signal at the given m/z of the organic mass spectra derived from ACSM observation results. The organic aerosols of these two pollution cases (July 30 and Aug 3) both had higher values of $f_{44}$, thus were more oxidized and aged, which was caused by extensive oxidation processes. These sulfate-dominated pollution episodes in the NEC are likely to be caused by regional transport due to extremely aged secondary aerosols while relatively lower values of $f_{44}$ and SOR together with notable fraction of HOA during clean situations indicate the importance of local sources.

Among these aircraft experiments, flight on July 30 was designed to investigate the role that mid-latitude cyclone plays in transporting air pollution and the aerosol chemistry alongside. Here we present the detailed analysis and in-depth understanding of this regional transport air pollution.

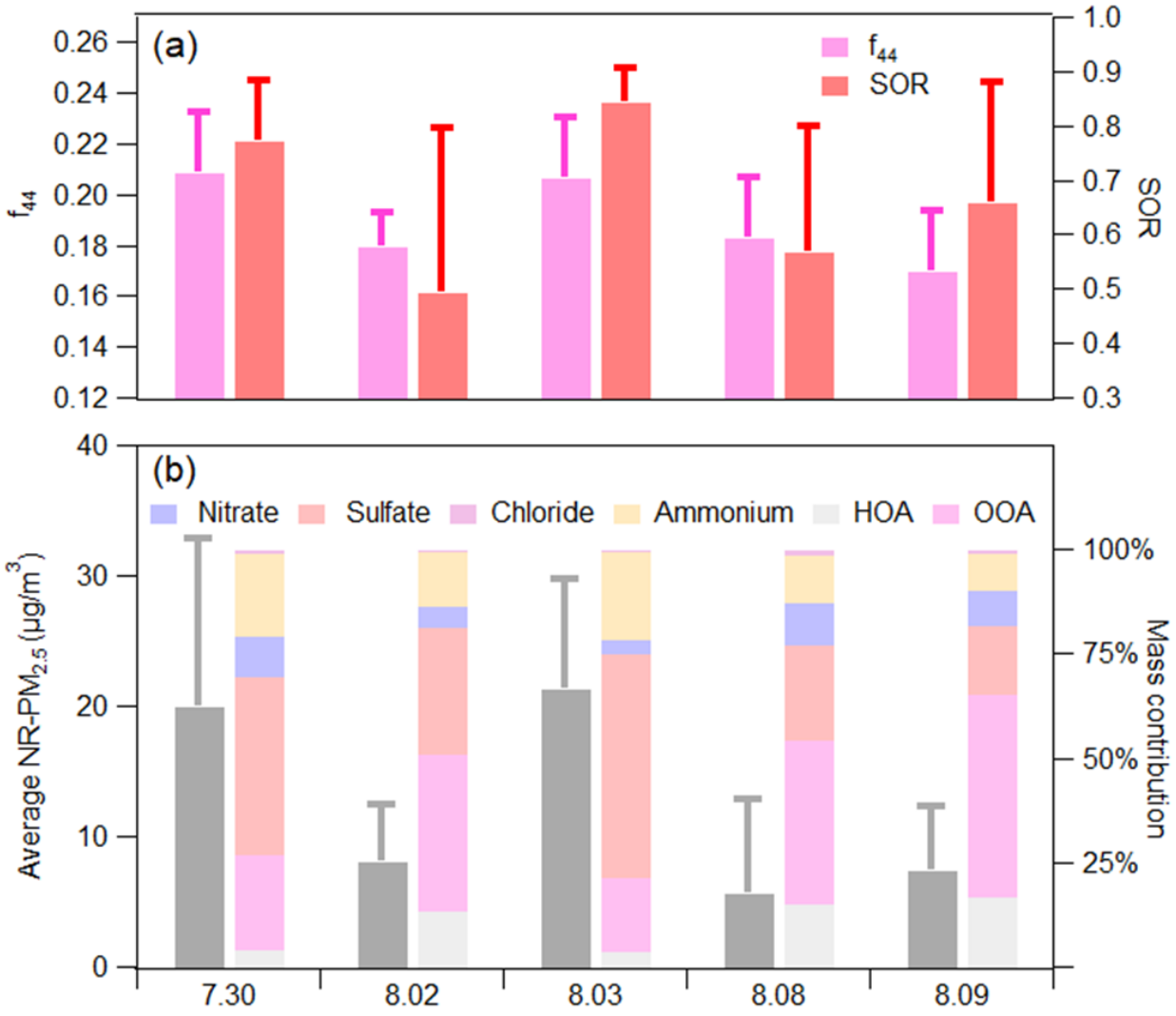


**Figure 2** Averaged (a) $f_{44}$ of organic aerosols and sulfur oxidation ratios; (b) NR-$PM_{2.5}$ mass concentrations and contributions from different aerosol species of each aircraft experiment.

3.2 Air pollution in free troposphere

On July 30, the aircraft ascended from the airport in Baicheng and made a clockwise flight in the North of the province at an altitude of around 2.5 km corresponding to the flight route in Fig. 1b and Fig. 3a. To capture the vertical distributions of air pollutants, the aircraft descended to about 1 km over the

two nearby cities, Daan and Songyuan, as shown in Fig. 3a. The flight was carried out from 12:30 to 16:50 LT on 30 July and covered about 500 km in total distance with the horizontal speed of nearly 200 km per hour.

Fig. 3b shows the time series of $SO_2$, $O_3$, $B_{sp}$, and NR-$PM_{2.5}$ and the flight altitude during the aircraft experiment on July 30. $B_{sp}$ and NR-$PM_{2.5}$ tracked each other well and both varied substantially between different altitudes. Organic aerosols dominated NR-$PM_{2.5}$ compositions within the PBL, the height of which can be derived from the vertical profile of temperature, which shows an obvious inversion layer at 1 900 m altitude (Fig. 4a). Once into the free troposphere, both ozone and NR-$PM_{2.5}$ mass concentrations showed sharp increases. Four pollution hot spots were observed during the flight, marked as A, B, C and D in Fig. 3a. Three of the plumes distributed around 1 ~ 2 km (defined as the Lower Free Troposphere (LFT)) above the cities of Baicheng, Daan and Songyuan, indicating the existence of pollution layer near the top of the PBL. Elevated pollution layers above PBL were also reported in previous aircraft studies (Ding et al., 2009; Liu et al., 2018; Sarangi et al., 2016), attributed to the regional transport. The fourth pollution hot spot was captured in the Higher Free Troposphere (HFT), e.g., ~ 3 km above Baicheng city, at 16:15 LT, marked as "D" in Fig. 3. Air pollutant levels were relatively low above 3.3 km.

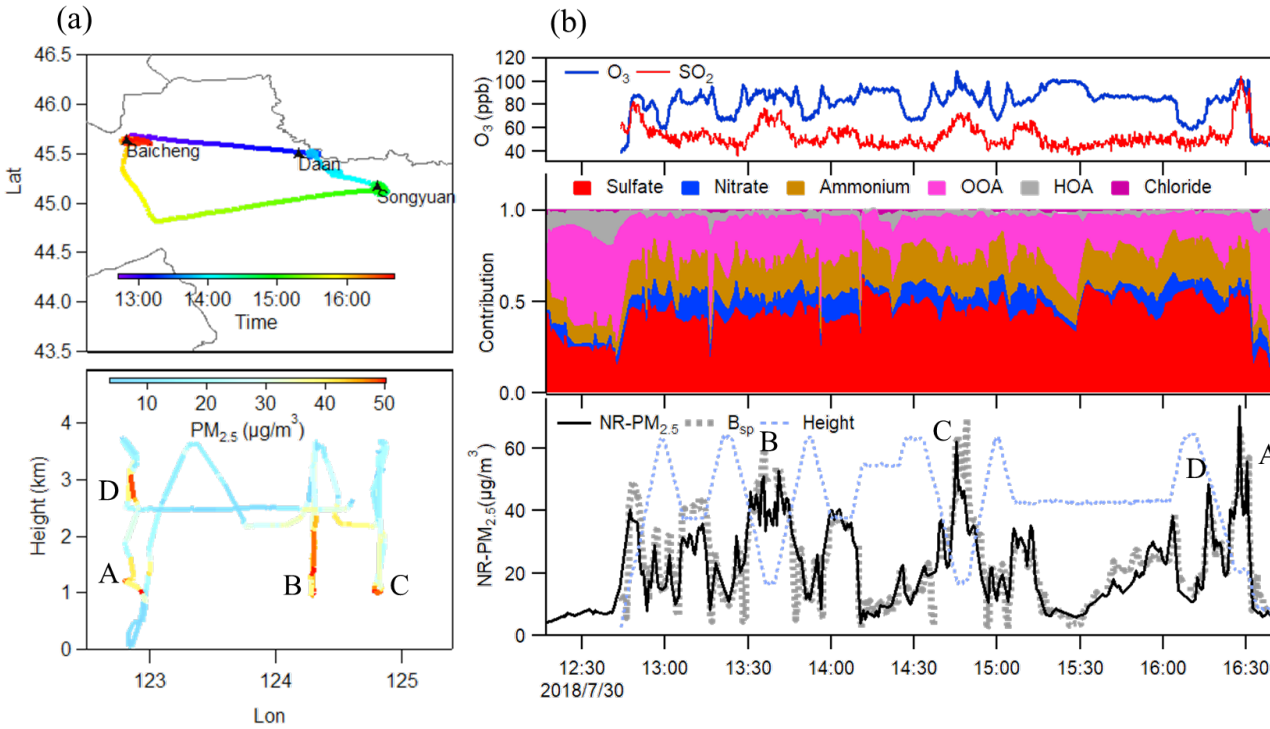


**Figure 3** (a) The flight track of July 30, 2018 over the NEC. The top panel is

color-coded by the local time and the bottom panel by the mass concentrations of NR-$PM_{2.5}$. (b) Time series of NR-$PM_{2.5}$ mass concentrations, Bsp, flight altitude, the mass contribution of different species to total NR-$PM_{2.5}$, $SO_2$ and $O_3$ mixing ratios during the flight on 30 July 2018. The corresponding $PM_{2.5}$ mass peaks were marked with A B C D in both (a) and (b) panels.

Fig. 4a presents the vertical profile of NR-$PM_{2.5}$ from 16:10 LT to 16:50 LT. NR-$PM_{2.5}$ was well-mixed within the PBL with a relative low concentration of ~8 μg $m^{-3}$ and a composition dominated by organics (65% of NR-$PM_{2.5}$ mass; Fig. 4c). HOA accounted for 25% of the OA mass within the PBL, indicating the importance of local sources in aerosol loadings in the PBL. A dramatic variation of aerosol mass concentration and composition was observed in the free troposphere, where high NR-$PM_{2.5}$ mass concentration of up to 74 μg $m^{-3}$ was observed with sulfate being the dominant component (48% of NR-$PM_{2.5}$ mass). An extremely low fraction of HOA (2% of NR-$PM_{2.5}$ mass) in both LFT and HFT suggested that the pollution plumes in the free troposphere were not contributed by local sources, but by regional transport instead. The aerosols in both LFT and HFT had substantially higher value of $f_{44}$ and SOR, indicative of secondary aerosols undergone extensive atmospheric processing and being aged before transported to the free troposphere. Note that the vertical distribution of aerosol composition observed in this study was different from that acquired by an aircraft study conducted in the NCP, a major pollution source region in China, where high levels of aerosols were trapped inside the PBL and were dominated by organics (Liu et al., 2019).

$SO_2$ can be oxidized into sulfate through multiple chemical pathways, i.e., gas-phase oxidations, aqueous phase reactions, and heterogeneous reactions (Seinfeld and Pandis, 2006). The geographical distribution of $SO_2$ concentrations (Fig. 1a) reveals that the flight reported here was carried out in a regional plume in the NEC due to relatively low emissions of $SO_2$ over the flight region. The distribution of the surface $PM_{2.5}$ mass concentrations during the flight time also denoted the influence of regional transport (Fig. S6) since the hot spots of $PM_{2.5}$ were mainly located to the south of the flight path.

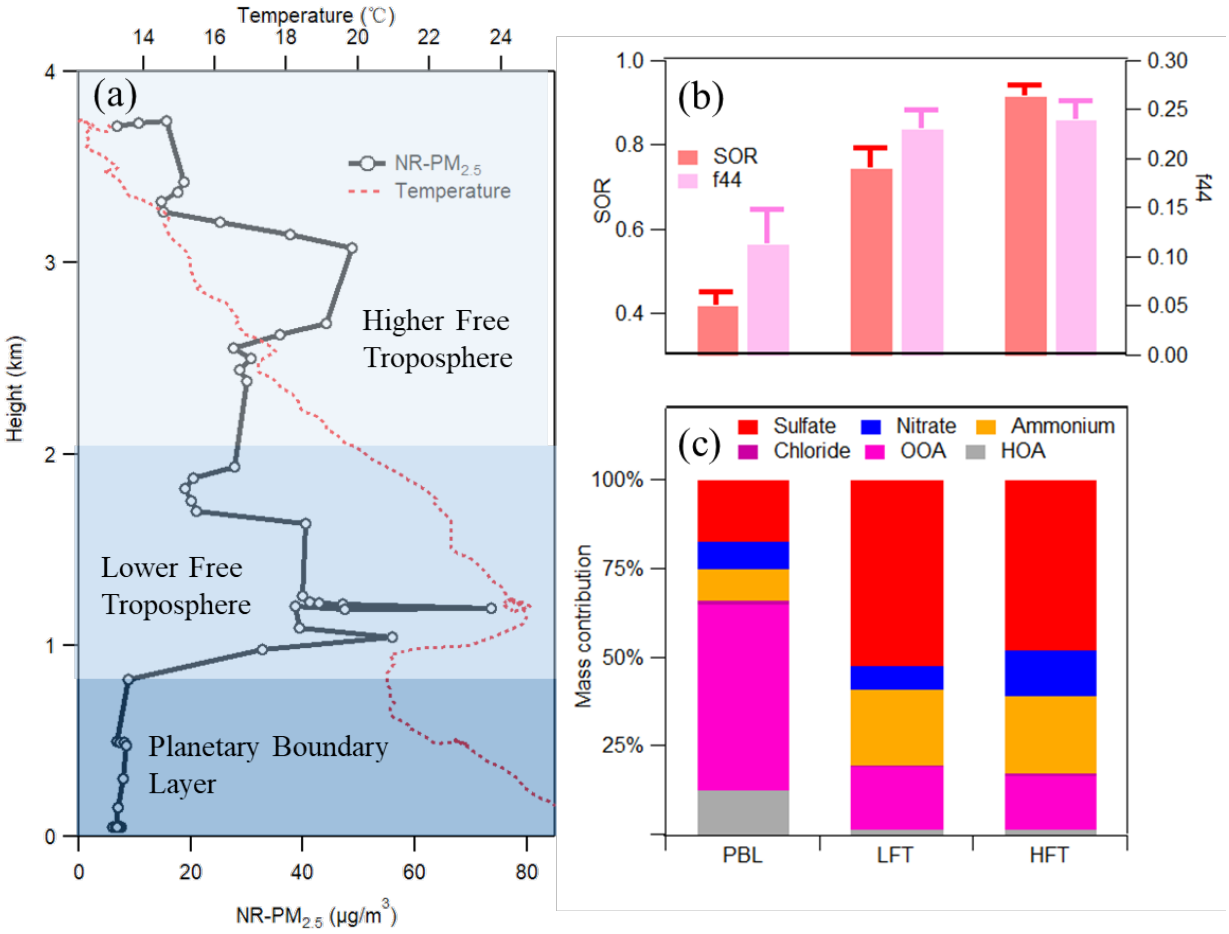


**Figure 4** (a) vertical profile of mass concentrations of NR-$PM_{2.5}$ and temperature; (b) sulfate conversion ratio (SOR) and $f_{44}$ of organic aerosols; (c) averaged contributions of NR-$PM_{2.5}$ species in the boundary layer (altitude below 900 m), the lower free troposphere (altitude from 900 m to 2000 m), and the higher free troposphere (altitude above 2000 m).

3.2 Regional transport associated with the synoptic processes

To identify the polluted plume sources and investigate their transport pathways, we conducted LPDM for the case on July 30, 2018. The upper panel of Fig. 5 shows that the air masses arriving at the lower free troposphere of all three cities including Baicheng, Daan, and Songyuan mainly originated from north Beijing and Hebei province, corresponding to the areas with high $PM_{2.5}$ loadings as shown in Fig. S6. As a comparison, air masses on the ground surface (blow 100 m) were mainly from local and transported from nearby northern clean region (Fig. 5d), resulting in the low aerosol loadings within the PBL.

Air stream pattern at 1 km altitude was analyzed using the ERA-5 reanalysis data to address the influence that the synoptic system has on air pollution transport. As shown in Fig. 6a, there were no prominent air flows from north Hebei Province directly to the aircraft flight area before the warm front. However, continuous southwestern winds brought water vapor to the NE China from the NCP after the warm front and led to the relatively high specific humidity over the study region (Fig. 6b). The high relative humidity (close to 100%) observed at the top of PBL (Fig. S7) further confirmed the influence of the water vapor. Warm and moist air masses was frequently observed at 900 hPa during the summer monsoon (Chen et al., 2020a). They were responsible for bringing pollutants of north Hebei directly to the NE China and formed a pollution layer in the lower troposphere, which was captured by our aircraft measurements. In addition, this water channel characterized by high specific humidity may also favor the formation of sulfate through aqueous phase processes (Xue et al., 2019).

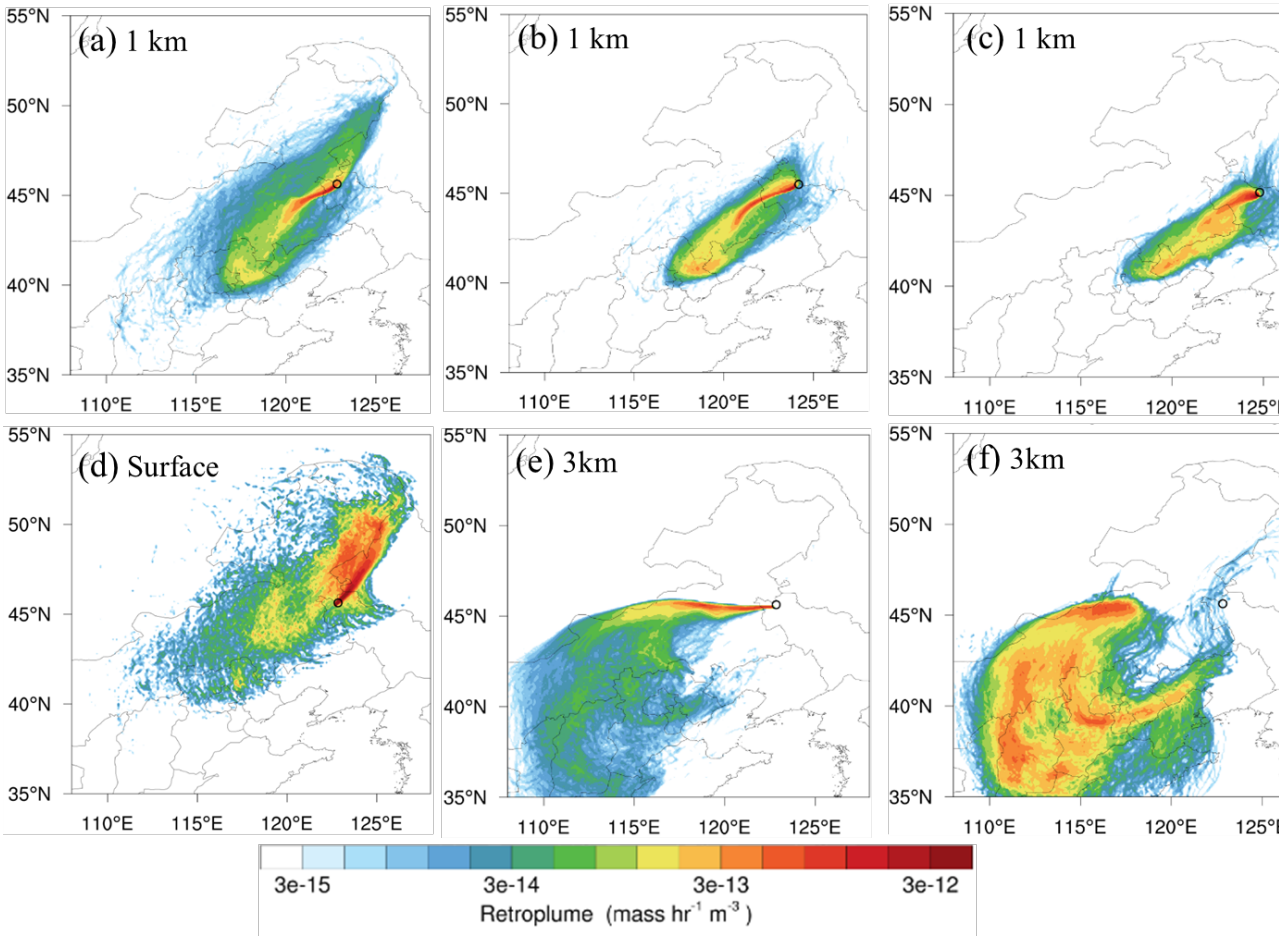


**Figure 5** 5-day retroplume (1 km footprint) for a receptor at an altitude of

1 km above (a) Baicheng; (b) Daan and (c) Songyuan corresponding to "A", "B", "C" as marked in Fig. 3. (d) 5-day retroplume (i.e., 100 m footprint) for a receptor at an altitude of 100 m above Baicheng sites; (e) 5-day retroplume (3 km footprint) and (f) 5-day retroplume (100 m footprint) for a receptor at an altitude of 3 km above Baicheng sites at 16: 00 LT on 30 July.

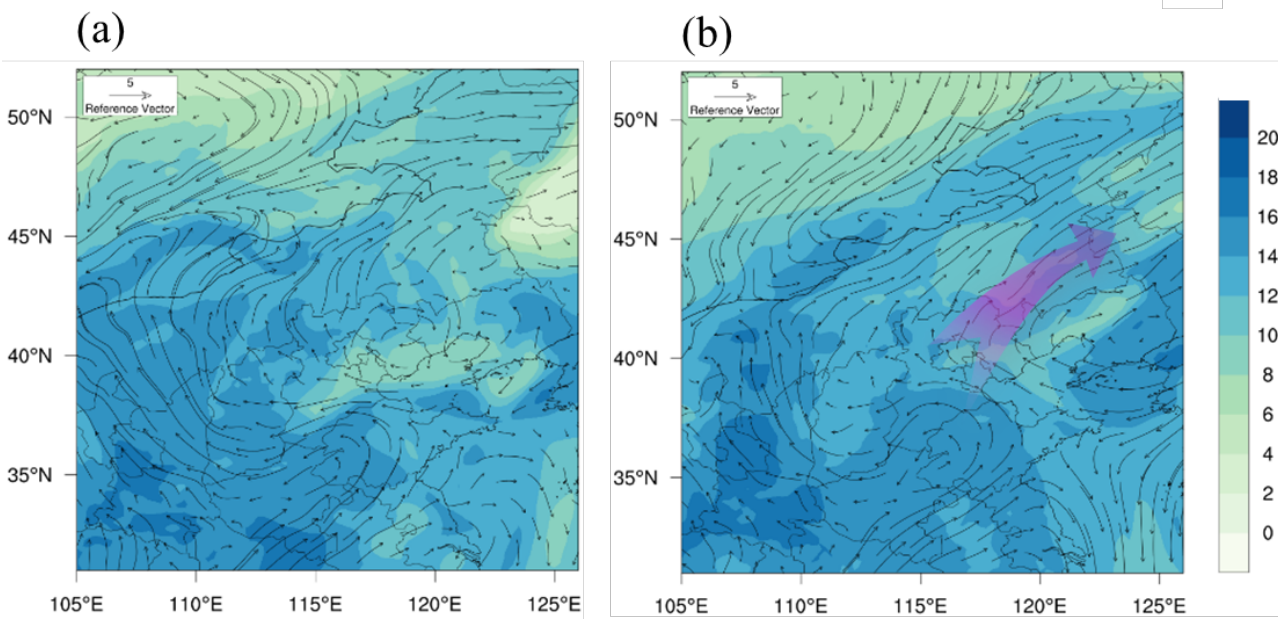


**Figure 6** Map showing the spatial distributions of specific humidity and wind vector at 900 hPa for (a) the time before the warm front; (b) the averaged time from 7.28 to 7.30. The purple arrow symbolizes the air masses transported from the NCP to the NEC. The meteorology data were from the ERA5 reanalysis website.

Unlike the transport path of the pollution in the LFT, the particles in the HFT show high residence time of 3 km footprint over the west shallow belt of the receptor site (Fig. 5e), indicating the different source regions and the transport path of pollutions in the separate layers. The surface footprint (under 100 m altitude) showed a high residence time over the polluted NCP (Fig. 5f). By combining Fig. 5e and Fig. 5f, we inferred that pollutants in the NCP were transported by the northward air flow and elevated by the warm front. This transport pathway of the HFT pollution was close to the warm conveyor belt (WCB) circulation, as shown in Fig. S1. In addition, the similar LPDM analysis conducted for pollution episode on August 3 also shows that the air masses arriving at the free troposphere in the NEC mainly originated from the NCP as shown in Fig. S11. Our results highlight the important role of regional transport from NCP in these sulfate-dominate air pollution episodes in the NEC.

To further investigate the role of the WCB in transporting pollutants from the NCP to the NEC, we simulated this frontal process using the WRF-Chem model. The simulated vertical distribution of sulfate mass concentrations was compared with that from our aircraft observations in Fig.S5. The observed pollution hot spot D in the HFT pollution was captured well by the model, while sulfate concentrations in the LFT were underestimated, possibly due to the the influence of high humidity air plumes. The uncertainties of uptake coefficient ( ) associated with relative humidity, aerosol liquid water content, particulate acidity and other factors in the model usually cause the discrepancy of secondary inorganic aerosols (Liu et al., 2021).

As shown in Fig. 7a, a high level of sulfate originated from the NCP (Shandong Province and Beijing) was transported northwardly towards the warm frontal region. The pollution plume was then lifted over the convergence belt, leading to high sulfate mass loadings at 2.6 km altitude (Fig. 7b). After that, this pollution plume was further transported horizontally to our aircraft site by strong westerly winds (Fig. S8). A process diagnostic analysis technique, as elaborated in Text S4, was applied to disentangle each individual contribution from different physical or chemical processes to sulfate variations over the study period. To get more insight into the pollution structure of WCB, the cross-section profiles of the contributions of chemical and advection processes to sulfate production are shown in Fig. 7c and d. The chemical formation of sulfate mainly occurred within the PBL from the ground to nearly 1 km with large values occurring over Beijing. However, high contribution of advection transport to sulfate concentrations occurred in the free troposphere caused by strong vertical wind. When the warm air masses arrived at the frontal region, pollutants were lifted by the strong updrafts (Fig. 7d). The sulfate chemically formed within the PBL in the NCP was thus lifted and transported to the NEC. These vertical structures clearly depicted the PBL-FT air pollution transport influenced by the WCB circulation. The diagnostic analysis also suggested that the increase of sulfate mass concentrations on July 30 in the HFT was attributed to the horizontal advection transport (Fig. S9).

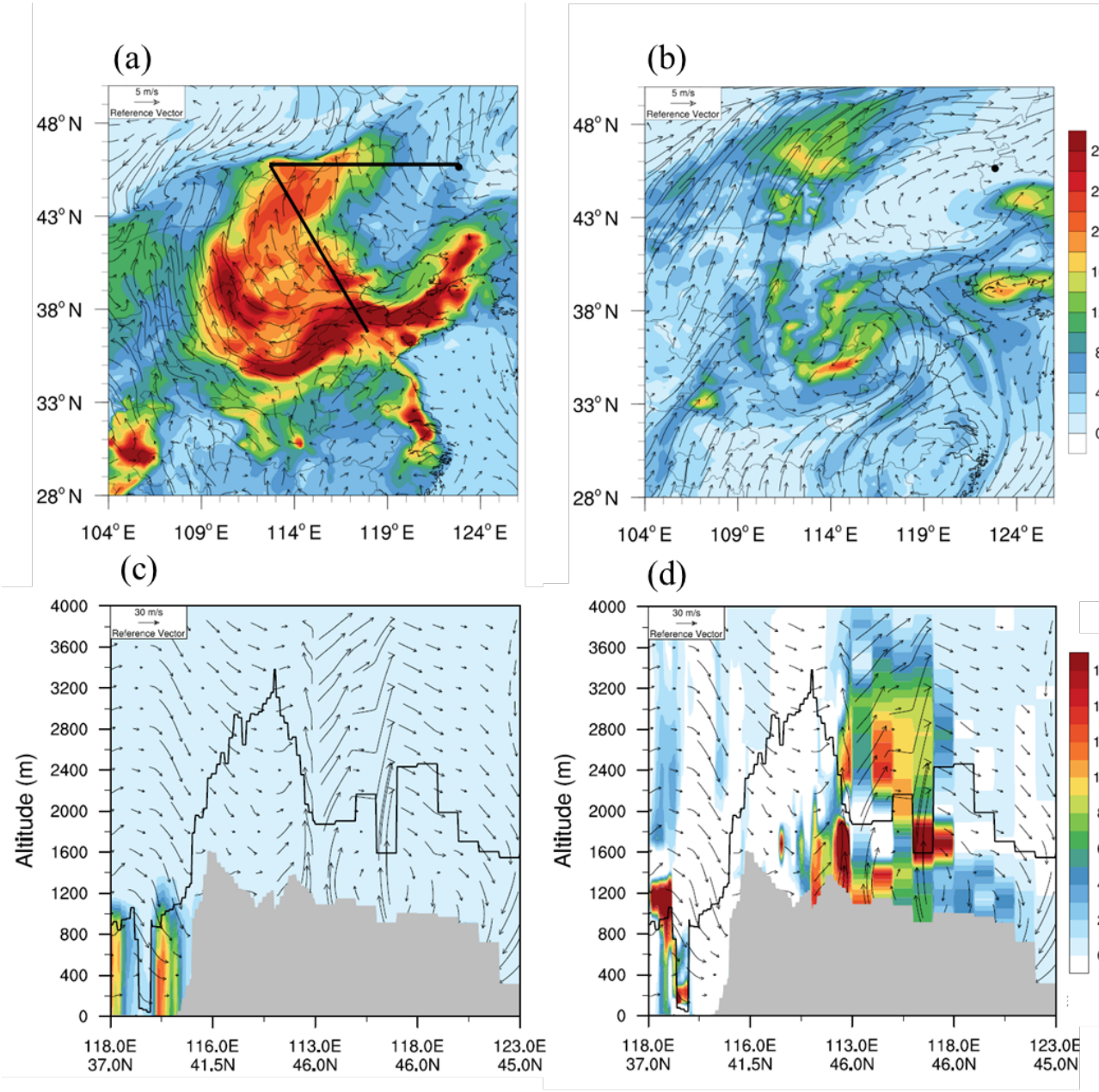


**Figure 7** Map showing the spatial distributions of (a) sulfate mass concentrations at the surface, (b) sulfate mass concentrations at 2.6 km altitude, and wind field at 16:00 local time on 28 July from WRF-Chem results. The contribution of (c) chemical production process (d) advection transport process on the vertical cross section of sulfate during the period with the warm front. The vertical

speed of in-plane wind vectors (arrows) was multiplied by a factor of 1800, and planetary boundary layer height was shown as the black solid line. The black solid line in panel (a) denotes the location of the vertical cross section shown in panel (c) and (d).

3.3 Evolution of aerosol chemistry during the regional transport

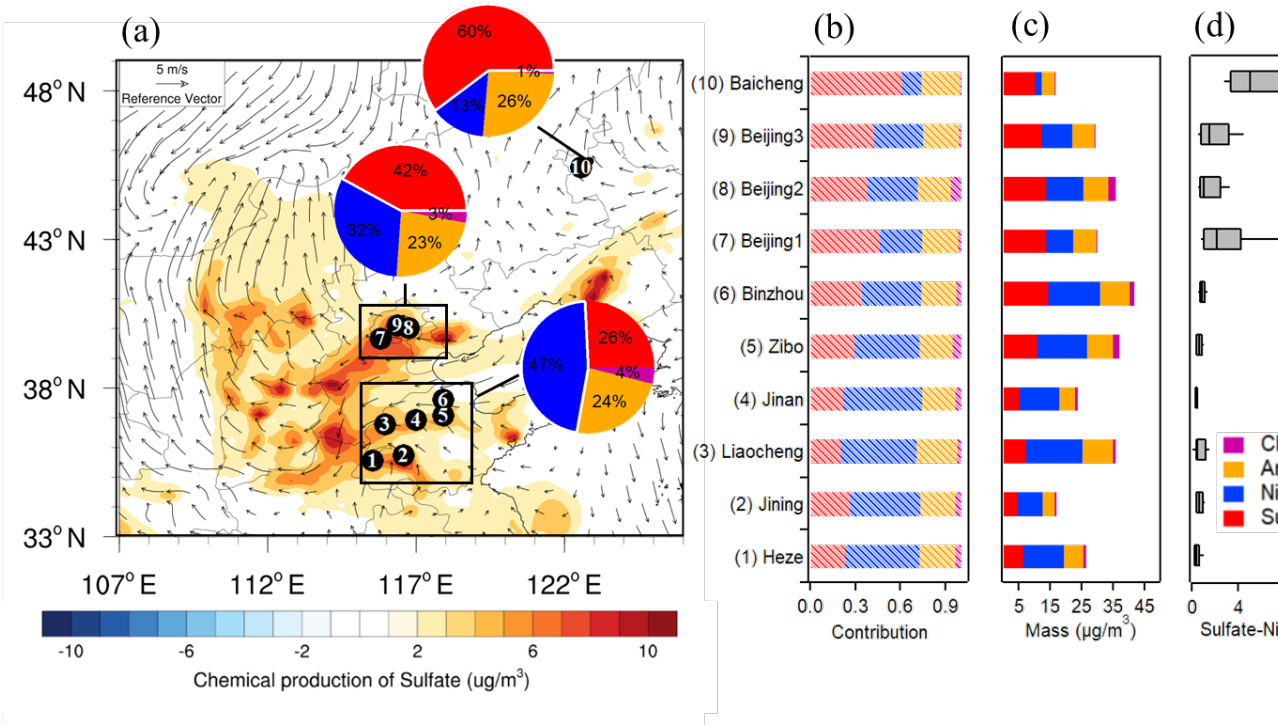


**Figure 8** (a) Map showing the spatial distributions of the chemical production of sulfate from July 27 to 28 from WRF-Chem results. The pie charts show the average contributions of different aerosol species during the same time for different regions from multiple observation results. The city names of each measurement site are marked with different numbers corresponding to the city numbers in the right panel. (b) average contributions of different aerosol species, (c) average concentrations of different aerosol species, (d) sulfate-to-nitrate ratio of different cities. All these results are based on ground online measurements except for Baicheng. The aircraft measurement data on July 30 was used to calculate the average aerosol compositions in Baicheng.

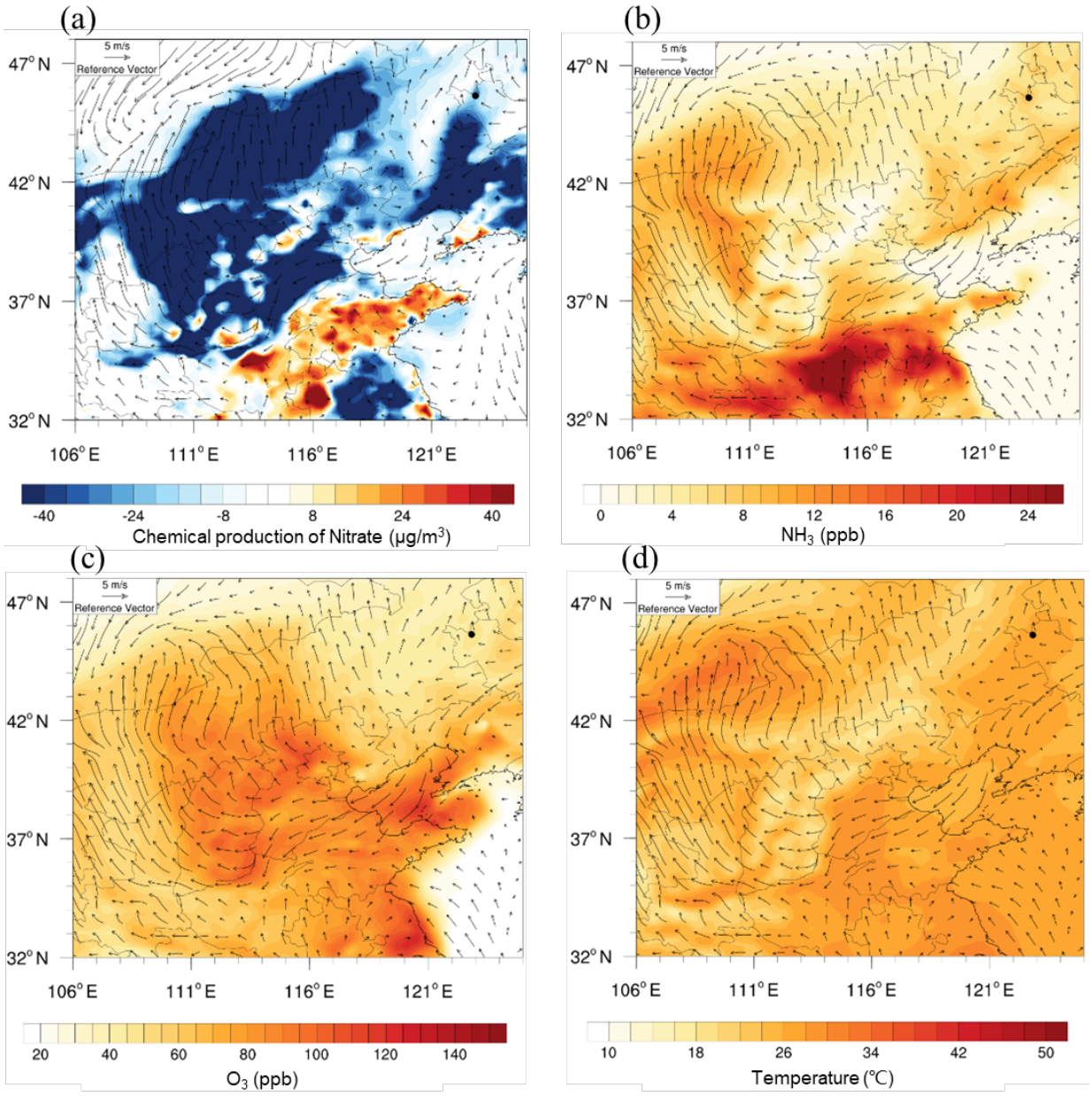


**Figure 9** Map showing the surface spatial distributions of (a) chemical production of nitrate, (b) average $NH_3$ mixing ratio, (c) average $O_3$ mixing ratio, (d) average temperature and Wind field from July 27 to 28.

Previous studies have shown that strong photochemical reactions and high temperature during summer favored the production of secondary aerosols in the

NCP, especially secondary inorganic aerosols (SNA) (Jiang et al., 2019; Li et al., 2017; Hu et al., 2017). However, the chemical evolution of aerosols during regional transport associated with synoptic systems has been rarely investigated. By combining multiple ground observations and the WRF-Chem model, we are able to perform an in-depth analysis of aerosol chemistry during the WCB transport. Note that the aerosol loadings here were indicated by the total mass concentrations of sulfate, nitrate, ammonium and chloride.

As shown in Figure 8a, a distinct transition of aerosol composition across multiple ground sites was observed during the regional transport. Both the mass concentrations and contributions of particulate nitrate decreased from south to north (Fig. 8c). Specifically, nitrate contributed a significant fraction of aerosol mass in Shandong (47%), while its contribution decreased to 32% in Megacity Beijing and eventually to 13% in the free troposphere in the NEC. In contrast, the contribution of particulate sulfate increased from the Shandong (26%) to Beijing (42%) and dominated NR-$PM_{2.5}$ (60%) in the NEC. Accordingly, sulfate-to-nitrate ratio depicted a significant increase during the WCB transport from Shandong to the NEC (Fig. 8d).

The transition of aerosol chemical compositions suggested the significant chemical processes occurring inside the air mass plume during the transport. Sulfate was strongly formed over the NCP, especially around Beijing (Fig. 8a), which was attributed to the high local primary emissions of $SO_2$ (Fig. S10) and the strong atmospheric oxidation capacity indicated by the high concentrations of $O_3$ (Fig. 9c). Similarly, particulate nitrate was largely formed over the Shandong due to high mixing ratios of $NO_2$ and $NH_3$ (Fig. 9b). Sulfate formation is irreversible and sulfate particles can be transported long-rangely without significant losses, whereas ammonium nitrate is a semi-volatile specie and can evaporate easily under high temperature, especially during summer (Feng and Penner, 2007). As a result, significantly negative nitrate chemical productions were observed over the north areas along the transport pathway of the WCB (Fig. 9a). Overall, the WCB circulations transported pollutants accumulated in PBL in the NCP to the FT in the NEC, during which an increasing contribution of sulfate to $PM_{2.5}$ was observed due to evaporation losses of ammonium nitrate.

Despite limited number of flight experiments conducted in the NEC, we have captured 2 sulfate-dominated pollution episodes. Our results indicate that the pollution accumulated in the NCP are easy to be transported to the NEC with secondary aerosols being oxidized and aged. Although particulate nitrate has been identified as the most important contributor to air pollution in China in recent years due to emission changes (Li et al., 2018; Sun et al., 2018; Ding et al., 2019), it may undergo evaporation loss during long-range transport, especially in summer, and thus sulfate becomes more important and serves as the driving factor of regional or trans-boundary pollution.

## 4. Conclusion

A multi-platform based campaign was organized using an aircraft in Northeast China (NE) and multiple ground observations in North China Plain (NCP), with the aim to investigate the role of mid-latitude cyclones in driving air pollutants from the NCP to the NEC, especially to understand the evolution of aerosol chemistry during the transport. Aircraft measurements showed relatively high aerosol loadings, dominated by sulfate in the free troposphere of the NEC despite low loadings of aerosols dominated by organics within the PBL. Lagrangian dispersion modeling and WRF-Chem simulation were conducted to understand the sources and transport characteristics of particulate pollution. Air pollution in the lower free troposphere was transported directly from north Hebei Province by warm and moist air masses at 900 hPa after the warm front. In contrast, pollution in the higher free troposphere was influenced by the warm conveyor belt, which transported particulate matters from the NCP and lifted them into the higher free troposphere. Both sulfate and nitrate formed intensively in the NCP but behaved differently during the transport to the north, in that sulfate concentrations stayed relatively constant while nitrate decreased readily due to evaporation losses. In addition to the well-understood regional transport processes from the NCP to the YRD (Sun et al., 2020), our results also identified the "chimney effect" imparted by the NCP, where aerosols are fast generated and blown by Asian monsoon to the YRD in winter when nitrate formation is favorable (Wang et al., 2020), and to the NEC in summer when nitrate formation is restricted.

Acknowledgments

This work was funded by the Ministry of Science and Technology of the People's Republic of China (2016YFC0200500), the National Natural Science Foundation of China (92044301) and High level personel project of Jiangsu Province (JSSCBS20210033). We thank colleagues at Jilin Provincial Weather Modification Office for their support on the aircraft field campaign, and those at Environmental Monitoring Centers in Shandong Province and Beijing for their contributions on the ground-based field measurements.

Data availability Statement

The emission data reported in Fig.1 are available at https://ladsweb.modaps.eosdis.nasa.gov/. All the meteorology data could be downloaded from the ERA 5 reanalysis website (https://cds.climate.copernicus.eu/cdsapp#!/dataset/reanalysis-era5-pressure-levels). All the aircraft and multiple ground measurement data used in this study are available at https://doi.org/10.5281/zenodo.5652522.

## References

Bethan, S., G. Vaughan, C. Gerbig, A. Volz-Thomas, H. Richer, and D. A. Tiddeman (1998), Chemical air mass differences near fronts, J Geophys Res-Atmos, 103(D11), 13413-13434.

Bao, M., et al. (2017), Characteristics and origins of air pollutants and carbonaceous aerosols during wintertime haze episodes at a rural site in the Yangtze River Delta, China, Atmospheric Pollution Research, 8(5), 900-911, doi:10.1016/j.apr.2017.03.001.

Chen, G. (2020a), Diurnal Cycle of the Asian Summer Monsoon: Air Pump of the Second Kind, J Climate, 33(5), 1747-1775, doi:10.1175/jcli-d-19-0210.1.

Chen, X., et al. (2020b), Common source areas of air pollution vary with haze intensity in the Yangtze River Delta, China, Environ Chem Lett, 18(3), 957-965.

Dickerson, R. R., et al. (2007), Aircraft observations of dust and pollutants over northeast China: Insight into the meteorological mechanisms of transport, J Geophys Res-Atmos, 112(D24).

Ding, A., T. Wang, and C. Fu (2013), Transport characteristics and origins of carbon monoxide and ozone in Hong Kong, South China, Journal of Geophysical Research: Atmospheres, 118(16), 9475-9488.

Ding, A., et al. (2009), Transport of north China air pollution by midlatitude cyclones: Case study of aircraft measurements in summer 2007, Journal of Geophysical Research, 114(D8).

Ding, A., et al. (2019), Significant reduction of PM2.5 in eastern China due to regional-scale emission control: evidence from SORPES in 2011–2018, Atmos Chem Phys, 19(18), 11791-11801.

Dong, X. Y., et al. (2018), Long-range transport impacts on surface aerosol concentrations and the contributions to haze events in China: an HTAP2 multi-model study, Atmos Chem Phys, 18(21), 15581-15600.

Du, H., et al. (2020), Effects of Regional Transport on Haze in the North China Plain: Transport of Precursors or Secondary Inorganic Aerosols, Geophys Res Lett, 47(14).

Ellison, E., L. Baker, and A. Wilson (2020), IPCC Special Report Meeting: Climate Change Around the Globe, Weather, 75(9), 293-294.

Feng, Y., and J. E. Penner (2007), Global modeling of nitrate and ammonium: Interaction of aerosols and tropospheric chemistry, J Geophys Res-Atmos, 112(D1).

Fröhlich, R., et al. (2013), The ToF-ACSM: a portable aerosol chemical speciation monitor with TOFMS detection, Atmospheric Measurement Techniques, 6(11), 3225-3241.

Grell, G., S. R. Freitas, M. Stuefer, and J. Fast (2011), Inclusion of biomass burning in WRF-Chem: impact of wildfires on weather forecasts, Atmos Chem Phys, 11(11), 5289-5303.

Henne, S., J. Dommen, B. Neininger, S. Reimann, J. Staehelin, and A. S. H. Prévôt (2005), Influence of mountain venting in the Alps on the ozone chemistry

of the lower free troposphere and the European pollution export, Journal of Geophysical Research, 110(D22), doi:10.1029/2005jd005936.

Hu, W., M. Hu, W.-W. Hu, J. Zheng, C. Chen, Y. Wu, and S. Guo (2017), Seasonal variations in high time-resolved chemical compositions, sources, and evolution of atmospheric submicron aerosols in the megacity Beijing, Atmospheric Chemistry and Physics, 17(16), 9979-10000.

Huang, R. J., et al. (2014), High secondary aerosol contribution to particulate pollution during haze events in China, Nature, 514(7521), 218-222.

Huang, X., Z. L. Wang, and A. J. Ding (2018), Impact of Aerosol-PBL Interaction on Haze Pollution: Multiyear Observational Evidences in North China, Geophys Res Lett, 45(16), 8596-8603.

Huang, X., A. Ding, Z. Wang, K. Ding, J. Gao, F. Chai, and C. Fu (2020), Amplified transboundary transport of haze by aerosol–boundary layer interaction in China, Nat Geosci, 13(6), 428-434.

Jiang, Q., F. Wang, and Y. Sun (2019), Analysis of Chemical Composition, Source and Processing Characteristics of Submicron Aerosol during the Summer in Beijing, China, Aerosol and Air Quality Research, 19(6), 1450-1462.

Jimenez, J. L., et al. (2009), Evolution of Organic Aerosols in the Atmosphere, Science, 326(5959), 1525-1529.

Kiley, C. M., and H. E. Fuelberg (2006), An examination of summertime cyclone transport processes during intercontinental chemical transport experiment (INTEX-A), J Geophys Res-Atmos, 111(D24).

Kim, H., Q. Zhang, G. N. Bae, J. Y. Kim, and S. B. Lee (2017), Sources and atmospheric processing of winter aerosols in Seoul, Korea: insights from real-time measurements using a high-resolution aerosol mass spectrometer, Atmos Chem Phys, 17(3), 2009-2033.

Kim, H., Q. Zhang, and J. Heo (2018), Influence of intense secondary aerosol formation and long-range transport on aerosol chemistry and properties in the Seoul Metropolitan Area during spring time: results from KORUS-AQ, Atmos Chem Phys, 18(10), 7149-7168.

Li, C., J. W. Stehr, L. T. Marufu, Z. Q. Li, and R. R. Dickerson (2012), Aircraft measurements of SO2 and aerosols over northeastern China: Vertical profiles and the influence of weather on air quality, Atmospheric Environment, 62, 492-501

Li, H., et al. (2017), Wintertime aerosol chemistry and haze evolution in an extremely polluted city of the North China Plain: significant contribution from coal and biomass combustion, Atmospheric Chemistry and Physics, 17(7), 4751-4768.

Li, H., Q. Zhang, B. Zheng, C. Chen, N. Wu, H. Guo, Y. Zhang, Y. Zheng, X. Li, and K. He (2018), Nitrate-driven urban haze pollution during summertime over

the North China Plain, Atmospheric Chemistry and Physics, 18(8), 5293-5306, doi:10.5194/acp-18-5293-2018.

Li, X. L., X. M. Hu, Y. J. Ma, Y. F. Wang, L. G. Li, and Z. Q. Zhao (2019), Impact of planetary boundary layer structure on the formation and evolution of air-pollution episodes in Shenyang, Northeast China, Atmospheric Environment, 214.

Li, Y. J., Y. Sun, Q. Zhang, X. Li, M. Li, Z. Zhou, and C. K. Chan (2017b), Real-time chemical characterization of atmospheric particulate matter in China: A review, Atmospheric Environment, 158, 270-304.

Liu, X., M. Chang, J. Zhang, J. Wang, H. Gao, Y. Gao, and X. Yao (2021), Rethinking the causes of extreme heavy winter PM2.5 pollution events in northern China, Science of The Total Environment, 794, doi:10.1016/j.scitotenv.2021.148637.

Paatero, P., and U. Tapper (1994), Positive Matrix Factorization - a Nonnegative Factor Model with Optimal Utilization of Error-Estimates of Data Values, Environmetrics, 5(2), 111-126.

Sarangi, C., S. N. Tripathi, A. K. Mishra, A. Goel, and E. J. Welton (2016), Elevated aerosol layers and their radiative impact over Kanpur during monsoon onset period, Journal of Geophysical Research: Atmospheres, 121(13), 7936-7957, doi:10.1002/2015jd024711.

Seinfeld, J. H., and Pandis, S. N. (2006), Atmospheric Chemistry and Physics: From Air Pollution to Climate 591 Change, John Wiley & Sons, New York, 2nd edition, 1232 pp., 13: 978-0-471-72018-8.

Stein, A. F., R. R. Draxler, G. D. Rolph, B. J. B. Stunder, M. D. Cohen, and F. Ngan (2015), Noaa's Hysplit Atmospheric Transport and Dispersion Modeling System, B Am Meteorol Soc, 96(12), 2059-2077.

Sun, P., et al. (2020), Impact of air transport and secondary formation on haze pollution in the Yangtze River Delta: In situ online observations in Shanghai and Nanjing, Atmospheric Environment, 225, 117350.

Sun, P., et al. (2018), Two years of online measurement of fine particulate nitrate in the western Yangtze River Delta: influences of thermodynamics and N2O5 hydrolysis, Atmos Chem Phys, 18(23), 17177-17190.

Sun, Y. L., Q. Jiang, Z. F. Wang, P. Q. Fu, J. Li, T. Yang, and Y. Yin (2014), Investigation of the sources and evolution processes of severe haze pollution in Beijing in January 2013, J Geophys Res-Atmos, 119(7), 4380-4398.

Sun, Y. L., Z. F. Wang, P. Q. Fu, T. Yang, Q. Jiang, H. B. Dong, J. Li, and J. J. Jia (2013), Aerosol composition, sources and processes during wintertime in Beijing, China, Atmospheric Chemistry and Physics, 13(9), 4577-4592.

ten Brink, H., R. Otjes, P. Jongejan, and S. Slanina (2007), An instrument for semi-continuous monitoring of the size-distribution of nitrate, ammonium,

sulphate and chloride in aerosol, Atmospheric Environment, 41(13), 2768-2779.

Qixin Tan, B. G., Xiaobin Xu, Lu Gan, Wenyi Yang, Xueshun Chen, Xiaole Pan, Wei Wang, Jie Li, Zifa Wang, (2021), Increasing impacts of the relative contributions of regional transport on air pollution in Beijing: Observational evidence, Environmental Pollution, doi:org/10.1016/j.envpol.2021.118407.

Ulbrich, I. M., M. R. Canagaratna, Q. Zhang, D. R. Worsnop, and J. L. Jimenez (2009), Interpretation of organic components from Positive Matrix Factorization of aerosol mass spectrometric data, Atmos Chem Phys, 9(9), 2891-2918.

Wang, J. D., et al. (2017), Particulate matter pollution over China and the effects of control policies, Sci Total Environ, 584, 426-447.

Wang, T., A. J. Ding, J. Gao, and W. S. Wu (2006), Strong ozone production in urban plumes from Beijing, China, Geophys Res Lett, 33(21).

Wang, T., X. Huang, Z. Wang, Y. Liu, D. Zhou, K. Ding, H. Wang, X. Qi, and A. Ding (2020), Secondary aerosol formation and its linkage with synoptic conditions during winter haze pollution over eastern China, The Science of the total environment, 730, 138888.

Wang, X., X. Ding, X. Fu, Q. He, S. Wang, F. Bernard, X. Zhao, and D. Wu (2012), Aerosol scattering coefficients and major chemical compositions of fine particles observed at a rural site in the central Pearl River Delta, South China, Journal of Environmental Sciences, 24(1), 72-77.

Wu, J. R., N. F. Bei, X. Li, J. J. Cao, T. Feng, Y. C. Wang, X. X. Tie, and G. H. Li (2018), Widespread air pollutants of the North China Plain during the Asian summer monsoon season: a case study, Atmos Chem Phys, 18(12), 8491-8504.

Xia, L., B. Zhu, H. Wang, H. Kang, and J. An (2020), Characterization and Source Apportionment of Fine Particles during a Heavy Pollution Episode over the Yangtze River Delta, China, Atmosphere, 11(7), doi:10.3390/atmos11070720.

Xue, J., X. Yu, Z. Yuan, S. M. Griffith, A. K. H. Lau, J. H. Seinfeld, and J. Z. Yu (2019), Efficient control of atmospheric sulfate production based on three formation regimes, Nat Geosci, 12(12), 977-982.

Xue, L., A. Ding, J. Gao, T. Wang, W. Wang, X. Wang, H. Lei, D. Jin, and Y. Qi (2010), Aircraft measurements of the vertical distribution of sulfur dioxide and aerosol scattering coefficient in China, Atmospheric Environment, 44(2), 278-282.

Zhang, J., et al. (2021), Trans-Regional Transport of Haze Particles From the North China Plain to Yangtze River Delta During Winter, J Geophys Res-Atmos, 126(8).

Zhang, Q., J. L. Jimenez, M. R. Canagaratna, I. M. Ulbrich, N. L. Ng, D. R. Worsnop, and Y. Sun (2011), Understanding atmospheric organic aerosols via

factor analysis of aerosol mass spectrometry: a review, Analytical and bioanalytical chemistry, 401(10), 3045-3067.

Zhang, Q., et al. (2007), Ubiquity and dominance of oxygenated species in organic aerosols in anthropogenically-influenced Northern Hemisphere midlatitudes, Geophys Res Lett, 34(13), n/a-n/a.

Zhang, R. Y., G. H. Wang, S. Guo, M. L. Zarnora, Q. Ying, Y. Lin, W. G. Wang, M. Hu, and Y. Wang (2015), Formation of Urban Fine Particulate Matter, Chem Rev, 115(10), 3803-3855.

Zhang, Y., A. J. Ding, H. T. Mao, W. Nie, D. R. Zhou, L. X. Liu, X. Huang, and C. B. Fu (2016), Impact of synoptic weather patterns and inter-decadal climate variability on air quality in the North China Plain during 1980-2013, Atmos Environ, 124, 119-128.

Zhou, W., W. Xu, H. Kim, Q. Zhang, P. Fu, D. R. Worsnop, and Y. Sun (2020), A review of aerosol chemistry in Asia: insights from aerosol mass spectrometer measurements, Environmental science. Processes & impacts, 22(8), 1616-1653.

## References from the Supporting Information

Huang, X., A. Ding, Z. Wang, K. Ding, J. Gao, F. Chai, and C. Fu (2020), Amplified transboundary transport of haze by aerosol–boundary layer interaction in China, Nat Geosci, 13(6), 428-434.

Ng, N. L., M. R. Canagaratna, J. L. Jimenez, Q. Zhang, I. M. Ulbrich, and D. R. Worsnop (2011), Real-Time Methods for Estimating Organic Component Mass Concentrations from Aerosol Mass Spectrometer Data, Environ Sci Technol, 45(3), 910-916.

Sun, P., et al. (2020), Impact of air transport and secondary formation on haze pollution in the Yangtze River Delta: In situ online observations in Shanghai and Nanjing, Atmospheric Environment, 225, 117350.

Wang, T., X. Huang, Z. Wang, Y. Liu, D. Zhou, K. Ding, H. Wang, X. Qi, and A. Ding (2020), Secondary aerosol formation and its linkage with synoptic conditions during winter haze pollution over eastern China, The Science of the total environment, 730, 138888.

Xu, W., P. Croteau, L. Williams, M. Canagaratna, T. Onasch, E. Cross, X. Zhang, W. Robinson, D. Worsnop, and J. Jayne (2016), Laboratory characterization of an aerosol chemical speciation monitor with PM2.5 measurement capability, Aerosol Science and Technology, 51(1), 69-83.